ground water

Static and Push–Pull Methods Using Radon-222 to Characterize Dense Nonaqueous Phase Liquid Saturations

by B.M. Davis[1,2], J.D. Istok[1], and L. Semprini[1]

Abstract

Naturally occurring radon in ground water can potentially be used as an in situ partitioning tracer to characterize dense nonaqueous phase liquid (DNAPL) saturations. The static method involves comparing radon concentrations in water samples from DNAPL-contaminated and noncontaminated portions of an aquifer, while the push-pull method involves the injection (push) and extraction (pull) of a radon-free test solution from a single well. In the presence of DNAPL, radon concentrations during the pull phase are retarded, with retardation manifested in greater dispersion of radon concentrations relative to a conservative tracer. The utility of these methods was investigated in the laboratory using a physical aquifer model (PAM). Static and push-pull tests were performed before and after contamination of the PAM sediment pack with trichloroethene (TCE), and after alcohol cosolvent flushing and pump-and-treat remediation. Numerical simulations were used to estimate the retardation factor for radon in push-pull tests. Radon partitioning was observed in static and push-pull tests conducted after TCE contamination. Calculated TCE saturations ranged up to 1.4% (static test) and 14.1% (push-pull test). Post-remediation tests showed decreases in TCE saturations. The results show that radon is sensitive to changes in DNAPL saturation in space and time. However, the methods are sensitive to DNAPL saturation heterogeneity, test location, sample size, and test design. The influence of these factors on test results, as well as the apparent overestimation of the retardation factor in push-pull tests, warrant further investigation.

Introduction

The release of nonaqueous phase liquids (NAPLs) to the subsurface environment can create long-term sources of ground water contamination as the NAPL slowly dissolves into ground water (Mercer and Cohen 1990; Cohen and Mercer 1993). Effective remediation of subsurface NAPL contamination requires that NAPL be accurately located and saturations quantified. This is particularly important for dense nonaqueous phase liquids (DNAPLs) because their high density causes them to migrate below the water table and move along pathways distinct from water flow (Schwille 1988; Nelson and Brusseau 1996).

Laboratory and field studies have shown that partitioning tracers can be used to locate and quantify NAPL contamination (Jin et al. 1995; Wilson and Mackay 1995; Nelson and Brusseau 1996; Annable et al. 1998; Nelson et al. 1999; Young et al. 1999). Partitioning tracers have the advantage of interrogating larger aquifer volumes compared to traditional coring techniques. These studies have typically involved the injection of a suite of conservative and partitioning tracers at one well, followed by the measurement of the tracers at one or more monitoring wells (i.e., an interwell tracer test). An alternative approach involves the use of single well "push-pull tests" in which the tracers are injected and extracted from the same well (Schroth et al. 2000; Davis et al. 2002). Retardation factors for injected partitioning tracers are determined from concentration breakthrough curves and, assuming linear equilibrium partitioning, NAPL saturations are calculated (see as follows).

Naturally occurring radon-222 (hereafter referred to as radon) can be used in lieu of injected partitioning tracers for locating and quantifying NAPL contamination. Radon is a naturally occurring, radioactive, inert isotope that occurs in ground water as a dissolved gas. A part of the uranium-238 decay series, radon has a half-life of 3.83 days and is continuously produced through the α-decay of radium-226

[1]Oregon State University, Department of Civil, Construction and Environmental Engineering, Corvallis, OR 97331; (541) 737–8870; fax (541) 737–3099; davisbri@engr.orst.edu

[2]Present address: Chevron Texaco Energy Research & Technology Co., 100 Chevron Way, P.O. Box 1627, Richmond, CA 94802; (510) 242-1030; fax (510) 242-1380; bmda@chevrontexaco.com

Received April 2002, accepted November 2002.

(half-life of 1600 years) that is contained within the structure of aquifer minerals and/or exists as secondary mineral coatings.

Radon has previously been used to investigate ground water recharge rates (Hamada and Komae 1998), ground water residence times (Snow and Spalding 1997), and ground water discharge to the ocean (Cable et al. 1996). Studies have shown that radon can be used as a partitioning tracer to locate and quantify NAPL contamination (Semprini et al. 1993; Hopkins 1995; Gottipati 1996; Hunkeler et al. 1997; Semprini et al. 1998; Semprini et al. 2000; Davis et al. 2002). In ground water, the equilibrium or "background" radon concentration ($C_{w,bkg}$) is a function of the radium content (C_{Ra}) and radon emanation power (E_p) of the mineral phases and the bulk density (ρ_b) and porosity (n) of the aquifer (Semprini et al. 2000):

$$C_{w,bkg} = \frac{C_{Ra}E_p\rho_b}{n} \tag{1}$$

Values of $C_{w,bkg}$ are highly variable ranging to 270,000 pCi/L or more in public water supplies (Hess et al. 1985; National Research Council 1999). Radon is moderately volatile, with a dimensionless Henry's coefficient (H_{cc}) of 3.9 at 20ºC (Clever 1979). Radon has an affinity for partitioning into NAPL; the linear partition coefficient (K) for radon is defined as

$$K = \frac{C_n}{C_{w,n}} \tag{2}$$

where C_n is the concentration of radon in the NAPL phase, and $C_{w,n}$ is the concentration of radon in the aqueous phase in the presence of NAPL.

Both static and push-pull methods using radon as a partitioning tracer can be used to locate and quantify NAPL contamination. The static method involves calculating NAPL saturations from a comparison of radon concentrations in ground water samples obtained from NAPL-contaminated and noncontaminated portions of the same aquifer. This method assumes secular equilibrium between radon emanation and decay, equilibrium radon partitioning between the water and NAPL phases, and a constant background radon concentration (Semprini et al. 2000). In the presence of NAPL, radon will be distributed between the water and NAPL phases as described by

$$C_nS_n + C_{w,n}S_w = \frac{C_{Ra}E_p\rho_b}{n} \tag{3}$$

where S_n and S_w are the NAPL and water saturations in the pore space ($S_n + S_w = 1$). Assuming linear equilibrium radon partitioning of radon between NAPL and water (Equation 2), Equation 3 can be rearranged as

$$C_{w,n} = \frac{C_{Ra}E_p\rho_b/n}{1 + S_n(K - 1)} \tag{4}$$

which can be further rearranged to solve for the NAPL saturation

$$S_n = \left(\frac{C_{w,bkg}}{C_{w,n}} - 1\right)\left(\frac{1}{(K - 1)}\right) \tag{5}$$

where $C_{w,n}$ is the radon concentration in ground water in the NAPL contaminated zone and $C_{w,bkg}$ is the radon concentration in ground water in a "background" zone outside of the NAPL-contaminated zone or in the aquifer before NAPL contamination has occurred. The push-pull method consists of the injection (push) of a known volume of radon-free test solution containing a conservative tracer (i.e., bromide) into a single well, followed by the extraction (pull) of the test solution/ground water mixture from the same well (Schroth et al. 2000). Previous studies have shown that pull phase radon breakthrough curves show an increased dispersion relative to bromide due to retardation resulting from mass transfer of radon between NAPL and the test solution (Davis et al. 2002). NAPL saturations are determined by estimating the radon retardation factor (R) during the pull phase of the test, where $R > 1$ in the presence of NAPL. Assuming linear equilibrium partitioning the retardation factor for radon is (Dwarakanath et al. 1999)

$$R = 1 + \frac{KS_n}{S_w} \tag{6}$$

Once the retardation factor is known, the NAPL saturation can then be calculated via (Dwarakanath et al. 1999)

$$S_n = \frac{R - 1}{R + K - 1} \tag{7}$$

In this study, we evaluate the use of static and push-pull methods using radon as an in situ partitioning tracer to estimate TCE DNAPL (hereafter referred to as TCE) saturations in a laboratory physical aquifer model (PAM) after TCE contamination and remediation. Spatial and temporal changes in static radon concentrations are used to estimate changes in TCE saturations, and push-pull test radon retardation factors are used to estimate TCE saturations as a function of space and time and to estimate the efficacy of remediation.

Experimental Methods

Static and push-pull tests were performed in selected portions of a large-scale rectangular PAM (Figures 1 and 2; experimental timeline shown in Table 1). The PAM consists of an aluminum box with interior dimensions of 4 m (length), 2 m (width), and 0.2 m (depth). Constant head reservoirs are located at each end of the PAM. Perforated aluminum plates covered with stainless steel screens separate the sediment pack from the reservoirs. The water height in the reservoirs is controlled by standpipe/overflow systems. An array of fully penetrating wells is fitted into the bottom of the PAM. The PAM is covered with an aluminum lid that is clamped to a flange around the perimeter. Sampling ports are located in the lid; these ports consist of a brass fitting through which a needle can be inserted into the sediment pack below. A more extensive description of the PAM can be found in Humphrey (1992).

Figure 1. Photograph of physical aquifer model (PAM) used in laboratory tests.

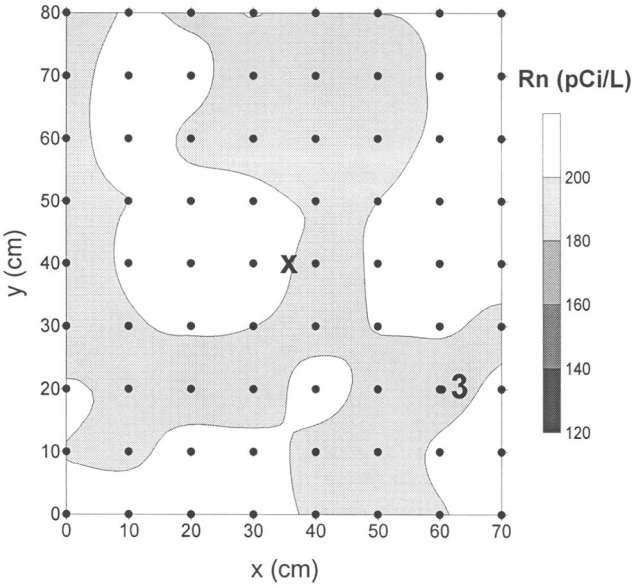

Figure 2. Plan view of portion of PAM used in laboratory tests, showing dimensions, fully penetrating well (x), sampling ports (●), and static radon concentrations prior to contamination of the PAM with TCE. Samples were obtained at a depth of 10 cm.

The PAM was packed using the method of Istok and Humphrey (1995) with sediment from the Hanford Formation, an alluvial deposit of sands and gravels of mixed basaltic and granitic origin (Lindsey and Jaeger 1993). The sediment was collected as a single batch from an outcrop at a quarry near Pasco, Washington. The sediment was homogenized by manual mixing, air-dried to a water content between 2 and 3 wt %, and sieved to remove particles >2 cm in diameter (which were <0.01% of the original outcrop material). The sieved sediment is a clean sand with ~30% fine gravels and <5% silt and clay. The sediment contains <0.001 wt % organic matter, and has a uniform bulk density (after packing) of 1.72 g/cm^3 and calculated porosity of 0.39. After sediment packing, the PAM was saturated with tap water from the constant head reservoirs, which was used as the synthetic ground water in all laboratory experiments.

For some tests, a portion of the sediment pack contained a known initial quantity of liquid TCE. This was achieved by slowly injecting aliquots of neat TCE at depths between 2.5 and 17.5 cm through 18 ports in the PAM lid (these ports do not correspond to the sampling ports described previously) using a 10 mL glass syringe (SGE, Ringwood, Australia) connected to a 12-gauge stainless steel needle (Aldrich Chemical, Milwaukee, Wisconsin). A total of 210.2 g (144 mL) of TCE was injected to create concentric zones of 6% and 3% TCE saturation (Figure 5). Following TCE injection, a push-pull test (described later) was conducted through the fully penetrating well to entrap TCE within the pore space (water samples were not obtained during this test).

Static and push-pull tests were performed under confined conditions. Each test was preceded by at least a three-week rest period during which radon concentrations reached >95% of their equilibrium value as a result of concurrent radon emanation from sediment and decay (Adloff and Guillaumont 1993). Static tests were performed under

Table 1

Experimental Timeline and Push-Pull Test Results, Showing Best Fit Radon Retardation Factors (R), Adjusted Retardation Factors, and TCE Saturations (S_n).

Test Type	Months After TCE Contamination	Figure	Test Location	Depth of Test (cm)	Volume Injected (L)	R	Adjusted R	S_n (%)
Static	—	2	sampling ports	10	—	—	—	—
Push-pull	—	3	sampling port 3	10	1.2	1.2	1.0	0
Push-pull	2	4	fully penetrating well	0–20	10	9.4	9.2	14.1
Static	3	5	sampling ports	10	—	—	—	-
Push-pull	8	6	fully penetrating well	0–20	10	3.8	3.6	4.9
Pull	9	7(a,b)	sampling ports and fully penetrating well	0–20	—	—	—	—
Static	20	8(a,b,c)	sampling ports	19.5	—	—	—	—
Static	25	9(a,b,c)	sampling ports	19.5	—	—	—	—
Push-pull	26	10	fully penetrating well	0–20	10	1.0	—	—
Push-pull	27	11	sampling port 1	19.5	1.2	7.0	6.8	10.4
Push-pull	27	12	sampling port 2	19.5	1.2	1.4	1.2	0.4

no-flow conditions by extracting 20 mL water samples through PAM sampling ports using a 20 mL plastic syringe (Becton-Dickinson, Franklin Lakes, New Jersey) attached to a 12-gauge stainless-steel needle that was inserted into the sediment pack through a sampling port.

Push-pull tests were performed (1) in a fully penetrating well located in the center of the TCE-contaminated portion of the PAM (Figure 2), and (2) in sampling ports using a 12-gauge stainless-steel needle inserted into the sediment pack. For the fully penetrating well tests, 10 L of test solution were injected and 20 L were extracted, while for the sampling port tests 1.2 L were injected and 2.4 L were extracted. Test solutions were injected and extracted using a piston pump (Fluid Metering, Oyster Bay, New York). The test solution consisted of tap water containing ~100 mg/L bromide, prepared from sodium bromide (Fisher Scientific, Fair Lawn, New Jersey) to serve as a conservative tracer. Dissolved radon was removed by bubbling compressed air through the test solution prior to injection. Injection and extraction pumping rates were constant at ~50 mL/min for the fully penetrating well tests and ~40 mL/min for the sampling port tests. Pull phase water samples were obtained using a 20 mL plastic syringe connected to a valve in a sampling line.

Time series concentration profiles of aqueous TCE and radon in the sediment pack after TCE contamination were obtained using a 15 L pull test (i.e., with no push phase preceding the pull phase) performed in the fully penetrating well. Water samples were obtained at depths of 7.5, 10, and 17.5 cm within the TCE-contaminated portion of the sediment pack using 20 mL plastic syringes and 12-gauge stainless-steel needles. Also, the fully penetrating well was used to obtain depth-integrated samples over the entire sediment pack.

Following a series of static and push-pull tests, ethanol cosolvent and tap water flushes were used to solubilize and remove TCE from the sediment pack. A 75% denatured ethanol (Fisher Scientific, Fair Lawn, New Jersey) solution was injected into the sediment pack (with four piston pumps) through four 12-gauge stainless-steel needles set within the TCE-contaminated portion of the PAM. The injection rate was 5 mL/min for each of the pumps. Another piston pump was used to simultaneously extract the ethanol solution/PAM water mixture through the fully penetrating well located at the center of the TCE-contaminated portion of the PAM. This pump was calibrated at 20 mL/min to create a steady-state flow regime in the PAM. A total of 89 L of ethanol solution were injected into the TCE-contaminated zone of the PAM. Following the ethanol flushes, ~1150 L of tap water (~ 2 pore volumes) were flushed through the PAM from the constant head reservoirs through the fully penetrating well. Water samples were obtained during the ethanol and tap water flushes using a 5 mL glass syringe (SGE, Ringwood, Australia) connected to a valve located in a sampling line. Static and push-pull tests were performed after remediation of the sediment pack.

The sediment pack was then drained and four core samples were obtained adjacent to the fully penetrating well. Each core sample was divided into three sections of equal length and each section placed in a 125 mL glass jar. Each jar was then filled with ~95 mL of methanol (Fisher Scientific, Fair Lawn, New Jersey), sealed, and placed on a mechanical shaker for 30 minutes. A 2 mL sample was collected by inserting a syringe needle through a septum in the jar lid and analyzed for methanol-extracted TCE.

Analytical Methods

Bromide concentrations were determined using a Dionex Model DX-120 ion chromatograph equipped with an electrical conductivity detector (Sunnyvale, California). Aqueous radon samples were filtered through a 2.0 µm filter (Millipore, Bedford, Massachusetts) attached to a syringe and a 1.5-inch steel needle (Becton-Dickinson, Franklin Lakes, New Jersey). The filtered sample (~15 mL) was then dispensed into the bottom of a pre-weighed 20 mL borosilicate scintillation vial containing 5 mL of Ultima Gold F scintillation "cocktail" (Packard Instruments, Meriden, Connecticut). Counting was performed with a Packard 2900 TR Liquid Scintillation Analyzer (LSA) as described by Cantaloub (2001). Aqueous TCE was quantified using a Waters HPLC using the method described by Field and Sawyer (2000), with a detection limit of 1 mg/L. The methodology of Cantaloub (2001) was used to determine the partition coefficient (K) for radon in the presence of TCE. This methodology incorporates a sequential liquid-liquid extraction technique using aqueous radium-226 and TCE. The radium-226 is used to generate radon-222. For each sequential extraction, an aliquot of TCE was added to a glass centrifuge tube containing aqueous radium-226, the solution was thoroughly mixed, and the TCE (now containing a proportion of the radon generated from the radium-226) removed. The TCE was then added to a liquid scintillation vial for counting. A value of $K = 50$ was determined, compared to a value of $K = 58$ for radon in the presence of trichloromethane (Clever 1979).

Data Analysis

Static radon data were used to calculate TCE saturations (S_n, Equation 5) after TCE contamination of the sediment pack, and after remediation. Radon and aqueous TCE concentrations and calculated values of S_n were plotted using the Surfer® software package (Golden Software, Golden, Colorado).

Push-pull test data analysis was performed using normalized bromide and radon concentrations. The normalized bromide concentration is defined as $C^* = 1–C/C_o$, where C is the measured bromide concentration in a sample and C_o is the bromide concentration in the injected test solution (~100 mg/L). This calculation is performed to facilitate the comparison of bromide and radon breakthrough curves. The normalized radon concentration is defined as $C^* = C_w/C_b$, where C_w is the measured radon concentration and C_b is the background radon concentration in the sediment pack, which was measured prior to each push-pull test. Push-pull tests were performed within less than eight hours so that radon emanation could be neglected. For each push-pull test, pull phase normalized radon and bromide concentrations were plotted as a function of dimensionless time V_e/V_i, where V_e is the volume of solution extracted from the sediment pack at the time a water sample was obtained, and

V_i is the total volume of solution injected into the sediment pack. Pull test radon and aqueous TCE concentrations were plotted as a function of the volume of solution extracted from the sediment pack at the time a sample was obtained.

Numerical simulations were performed with the Subsurface Transport Over Multiple Phases (STOMP) code, a fully implicit volume-integrated finite difference simulator (White and Oostrom 2000). Solute transport was simulated using PAM sediment pack properties for a range of retardation factors (R). The longitudinal dispersivity of the sediment pack was estimated for each push-pull test by fitting the experimental normalized bromide breakthrough curve to an approximate analytical solution for the pull phase of the test (Gelhar and Collins 1971; Schroth et al. 2000) as described by Davis et al. (2002). This dispersivity value was then used in the simulation of each push-pull test for a range of retardation factors (R) using STOMP, thus producing a series of simulated breakthrough curves. A least-squares method was used to determine which simulated breakthrough curve (corresponding to a specific value of R) best fit the experimental normalized radon breakthrough curve for each push-pull test. The value of S_n for the best fit value of R was then calculated using Equation 7.

Results

Prior to TCE contamination, static radon concentrations from samples obtained at a depth of 10 cm ranged from 181 to 224 pCi/L (Figure 2), with this variability likely due to heterogeneity of porosity and radon emanation in the sediment pack. Results from the pull phase of a push-pull test conducted prior to TCE contamination at a depth of 10 cm in sampling port 3 (location shown in Figure 2) are shown in Figure 3. Breakthrough curves are displayed as normalized concentration (C^*) versus dimensionless time (V_e/V_i) for bromide and radon. Normalized concentrations increased smoothly as the test solution was extracted from the sediment pack, and radon transport was slightly retarded relative to bromide. The normalized bromide concentration data were well fit by a simulated R = 1 breakthrough curve, while the normalized radon concentration data were best fit by a simulated R = 1.2 breakthrough curve (Table 1). Additional push-pull tests performed under the same conditions at different sampling ports (data not shown) showed results similar to Figure 3. Following these tests TCE was injected into the PAM sediment pack as described previously.

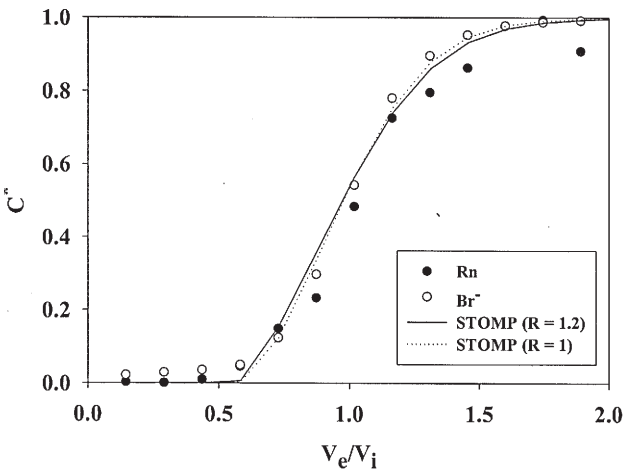

Figure 3. Pull phase breakthrough curves for a push-pull test conducted in sampling port 3 prior to contamination of the PAM with TCE. The test was conducted at a depth of 10 cm.

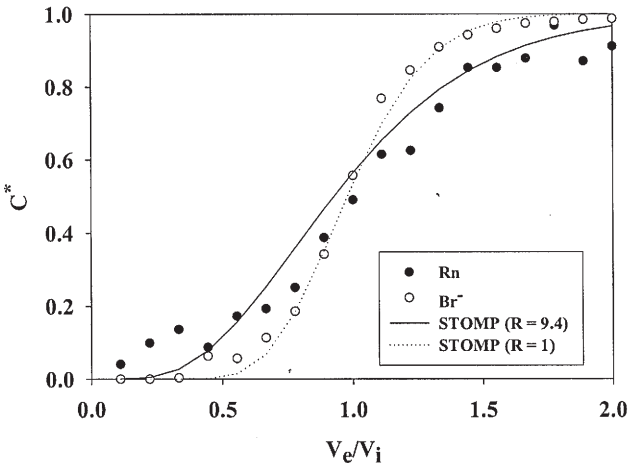

Figure 4. Pull phase breakthrough curves for the first push-pull test conducted in the fully penetrating well after contamination of the PAM with TCE.

Two months after TCE contamination, a push-pull test was conducted in the fully penetrating well. Normalized concentrations increased smoothly as the test solution was extracted from the sediment pack, and radon transport was retarded relative to bromide with the radon retardation manifested as greater dispersion relative to bromide (Figure 4). The normalized bromide concentration data were well fit by a simulated R = 1 breakthrough curve while the normalized radon concentration data were best fit by a simulated R = 9.4 breakthrough curve (Table 1). Another static test was then performed with radon samples again being obtained from a depth of 10 cm (Figure 5). Radon concen-

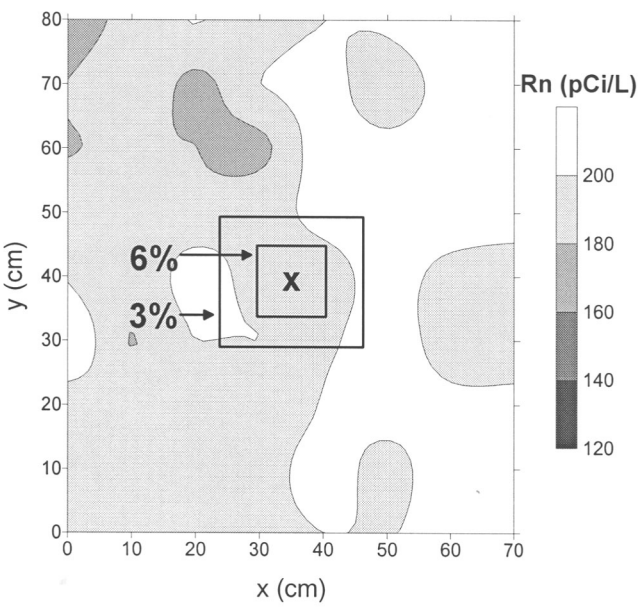

Figure 5. Plan view of static radon concentrations after contamination of the PAM with TCE. Samples were obtained at a depth of 10 cm.

trations ranged from 166 to 225 pCi/L. The radon retardation in the previous push-pull test, combined with the negligible change in static radon concentrations at the 10 cm depth relative to pre-contamination concentrations (Figure 2), supported a hypothesis that TCE had sunk to the bottom of the sediment pack. A second push-pull test was conducted in the fully penetrating well eight months after TCE contamination. Normalized concentrations increased smoothly as the test solution was extracted from the sediment pack, although the radon data exhibited some unexplained tailing at the end of the test (Figure 6). Radon transport was retarded relative to bromide, but to a lesser extent than the earlier test (Figure 4). The normalized bromide concentration data were well fit by a simulated $R = 1$ breakthrough curve while the normalized radon concentration data were best fit by a simulated $R = 3.8$ breakthrough curve (Table 1), compared to the larger best fit $R = 9.4$ for the first push-pull test in the fully penetrating well. The decrease in R between the two tests indicated a change in TCE saturation and is consistent with the hypothesis that TCE had sunk.

A 15 L pull test was then conducted to further investigate the TCE distribution in the sediment pack. Time series concentration profiles show that radon concentrations decreased with depth with the exception of the 7.5 cm depth (Figure 7a), where partitioning to a gas phase at the top of the sediment pack probably resulted in reduced concentrations. The decrease in radon concentrations between 3 and 5 L at the 17.5 cm depth likely results from water originating from a zone of high TCE saturation toward the bottom of the sediment pack. Aqueous TCE concentrations increased with depth and approached the solubility limit (~1000 mg/L) at 17.5 cm (Figure 7b), which correlates well with decreasing radon concentrations with depth to indicate that TCE had sunk to the bottom of the sediment pack.

Following the 15 L pull test, another static test was performed, with radon and aqueous TCE samples obtained at a depth of 19.5 cm. This depth was chosen to further investigate the hypothesis that TCE had sunk to the bottom of the sediment pack. Unfortunately, radon samples were not collected from this depth prior to TCE contamination. Due to partitioning into TCE, radon concentrations were

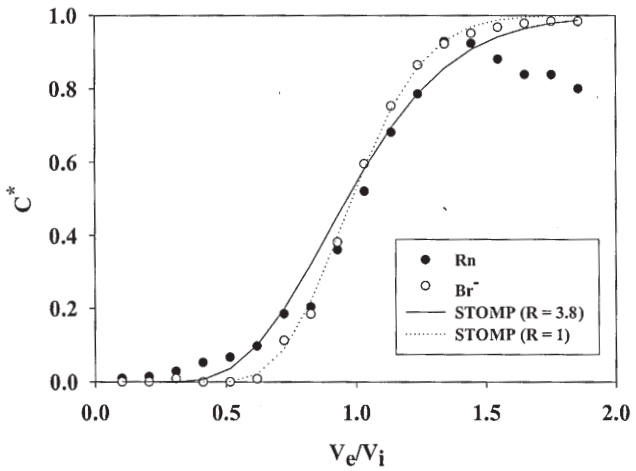

Figure 6. Pull phase breakthrough curves for the second push-pull test conducted in the fully penetrating well after contamination of the PAM with TCE.

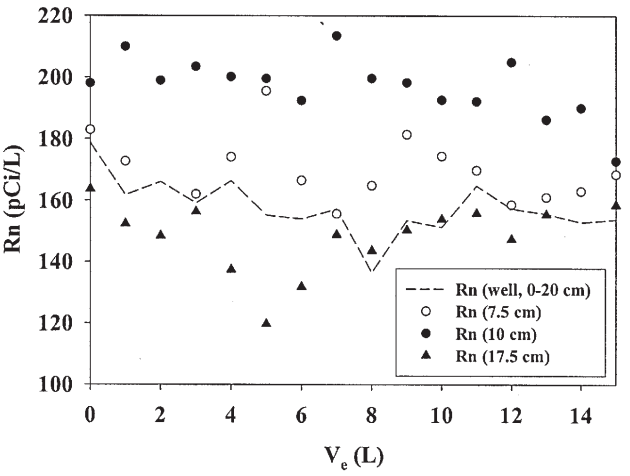

Figure 7a. Time series concentration profile of radon concentrations (pCi/L) for a pull test conducted after contamination of the PAM with TCE. Samples were obtained from the fully penetrating well (average = 157.7, standard deviation = 9.1), and from needles located at depths of 7.5 cm (average = 170.1, standard deviation = 10.6); 10 cm (average = 197.0, standard deviation = 9.6); and 17.5 cm (average = 147.5, standard deviation = 11.3).

reduced in the sediment pack, ranging from 120 to 217 pCi/L (Figure 8a), compared to the previous static test conducted at a depth of 10 cm (Figure 5). The greatest radon concentration reductions occurred in the vicinity of the concentric zones of 6% and 3% TCE saturation. Aqueous TCE concentrations ranged from 251 mg/L to the solubility limit, with the highest concentrations located in the 6% and 3% TCE saturation zones (Figure 8b). Calculated TCE saturations (S_n) show a maximum value of 1.4% (Figure 8c) in the vicinity of both the lowest radon concentrations and the highest aqueous TCE concentrations.

The TCE in the sediment pack was then remediated using a series of ethanol cosolvent and tap water flushes. Gross mass balance TCE calculations were performed

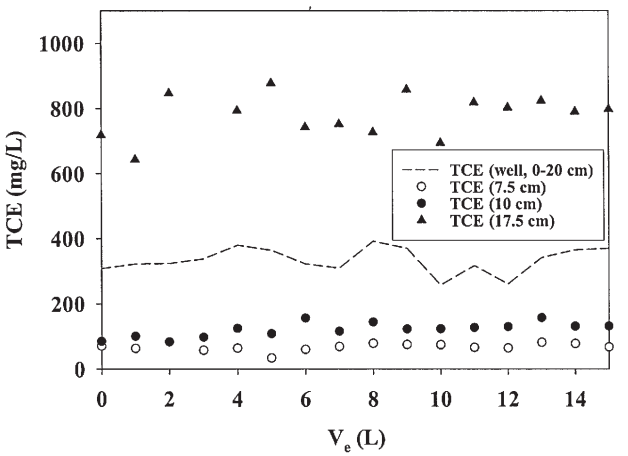

Figure 7b. Time series concentration profile of aqueous TCE concentrations (mg/L) for a pull test conducted after contamination of the PAM with TCE. Samples were obtained from the fully penetrating well (average = 334.1, standard deviation = 39.4), and from needles located at depths of 7.5 cm (average = 66.7, standard deviation = 11.5); 10 cm (average = 120.8, standard deviation = 22.1); and 17.5 cm (average = 779.6, standard deviation = 65.3).

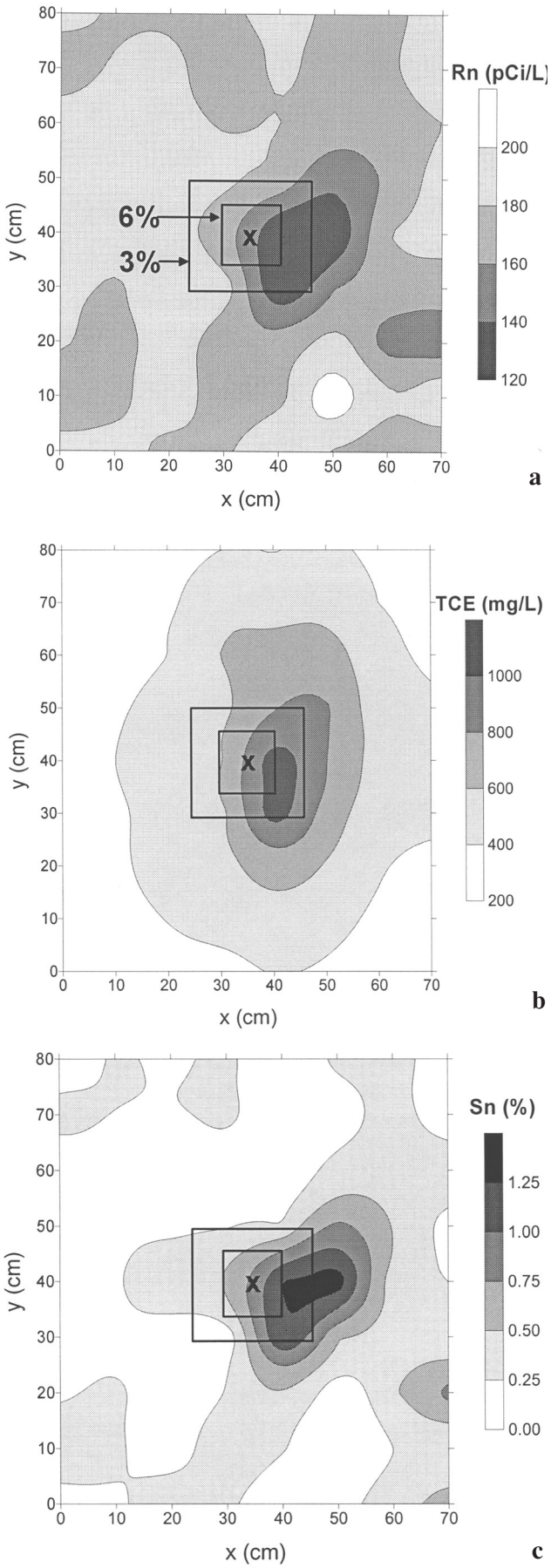

Figure 8. Plan view of (a) static radon concentrations, (b) static aqueous TCE concentrations, and (c) calculated TCE saturations (S_n) after contamination of the PAM with TCE. Samples were obtained from a depth of 19.5 cm.

using aqueous TCE data from the remediation activities and the 15 L pull and push-pull test immediately preceding remediation. These calculations showed that roughly 50% of the injected TCE was removed over the course of these experiments. However, the actual amount of TCE removed is likely >50% since additional push-pull tests were performed where aqueous TCE was not sampled. The remediation was followed by a three-week rest period to allow for the equilibration of radon concentrations in the pore water. Another static test was then performed at a depth of 19.5 cm. Radon concentrations increased across portions of the PAM and decreased in other locations (ranging from 140 to 219 pCi/L, Figure 9a) and aqueous TCE concentrations were decreased (ranging from <1 to 19 mg/L, Figure 9b). Calculated TCE saturations (S_n) show a maximum value of 1.3% in the vicinity of the lowest radon concentrations (Figure 9c), although aqueous TCE concentrations were <5 mg/L in this portion of the PAM.

Another push-pull test was then performed in the fully penetrating well. Normalized concentrations increased smoothly as the test solution was extracted from the sediment pack, although there is no clear evidence for radon retardation relative to bromide (Figure 10). The normalized bromide concentration data were not well fit by a simulated $R = 1$ breakthrough curve. The normalized radon concentration data were best fit by a simulated $R = 1$ breakthrough curve, although the fit is poor (Table 1). The normalized bromide and radon concentration data show increased dispersion compared to identical push-pull tests conducted before remediation (Figures 4 and 6), making breakthrough curve interpretation difficult.

Push-pull tests were then performed at a depth of 19.5 cm in sampling ports 1 (located in the TCE injection zone) and 2 (located outside the TCE injection zone, Figure 9a). These ports were chosen based on static sampling data (Figure 9c) which indicated that the sediment pack near sampling port 1 was contaminated with TCE, while there was a decreased likelihood of TCE contamination near sampling port 2. Unfortunately, push-pull tests were not performed in these sampling ports before remediation, which would have enabled a comparison of pre- and post-remediation radon retardation factors. For both push-pull tests normalized concentrations increased smoothly as the test solutions were extracted from the sediment pack (Figures 11 and 12). Radon transport was retarded relative to bromide in sampling port 1, and slightly retarded in sampling port 2. The normalized bromide concentration data were well fit by a simulated $R = 1$ breakthrough curve for both tests. The normalized radon concentration data were best fit by a simulated $R = 7$ breakthrough curve in sampling port 1 and simulated $R = 1.4$ breakthrough curve in sampling port 2 (Table 1). Following these push-pull tests, the PAM was drained and four core samples were obtained adjacent to the fully penetrating well. All core samples showed methanol-extracted TCE concentrations below detection limits (1 mg/L).

Discussion

Partitioning of radon between the pore water and trapped gas present in the sediment pack is likely the cause

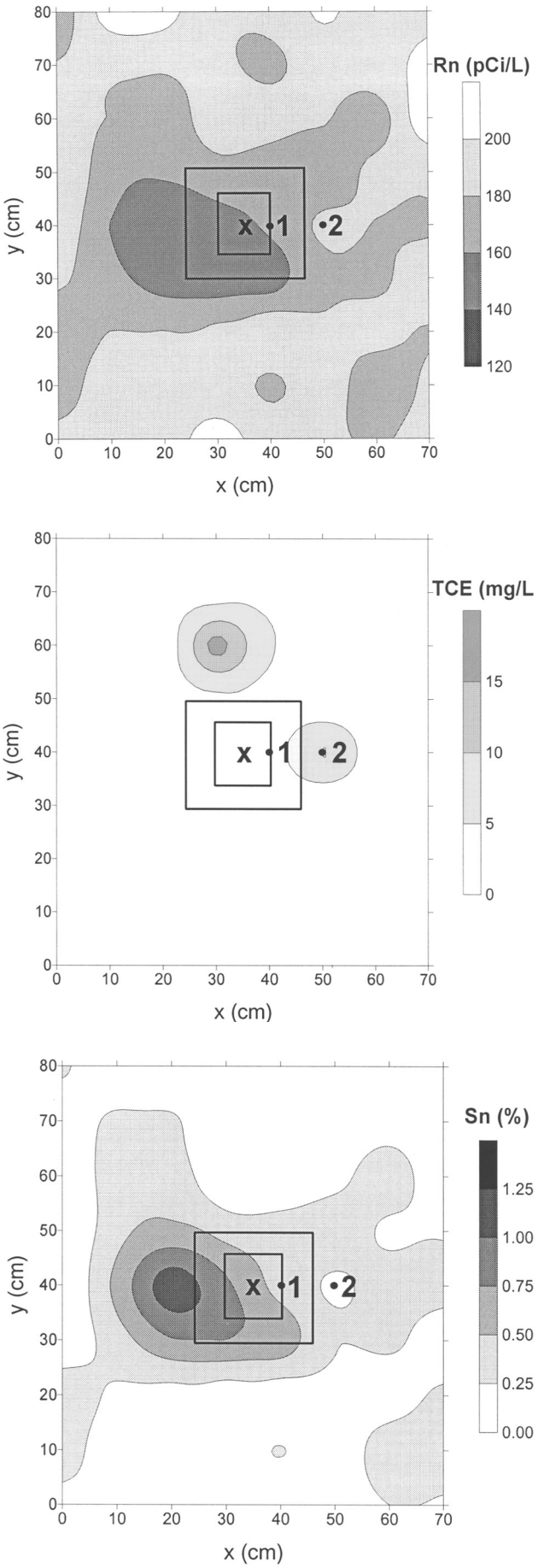

Figure 9. Plan view of (a) static radon concentrations, (b) static aqueous TCE concentrations, and (c) calculated TCE saturations (S_n) after PAM remediation. Samples were obtained from a depth of 19.5 cm.

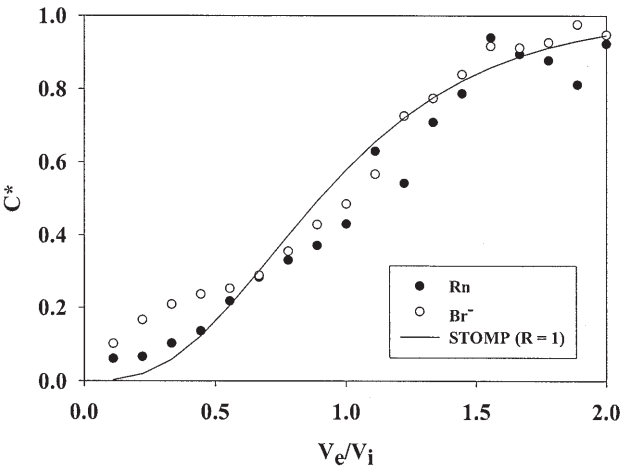

Figure 10. Pull phase breakthrough curves for the push-pull test conducted in the fully penetrating well after PAM remediation.

of the slight radon retardation observed in the push-pull test conducted prior to TCE contamination (Figure 3). This phenomenon has been observed in previous laboratory push-pull tests using the same sediment (Davis et al. 2002). Assuming equilibrium partitioning between the trapped gas and aqueous phases, the retardation factor for a dissolved gas can be written as (Fry et al. 1995)

$$R = 1 + H_{cc}\frac{S_g}{S_w} \tag{8}$$

where H_{cc} is the dimensionless Henry's constant and S_g is the trapped gas saturation. Using Equation 8, a value of H_{cc} = 3.9 for radon (Clever 1979), and the best fit R = 1.2 for radon from the push-pull test, the estimated gas saturation in the sediment pack is 5%.

Radon retardation during the push-pull tests conducted after TCE contamination was likely due to (1) radon partitioning between TCE and the aqueous phase, and (2) radon partitioning between trapped gas and the aqueous phase. In order to estimate the portion of radon retardation due to

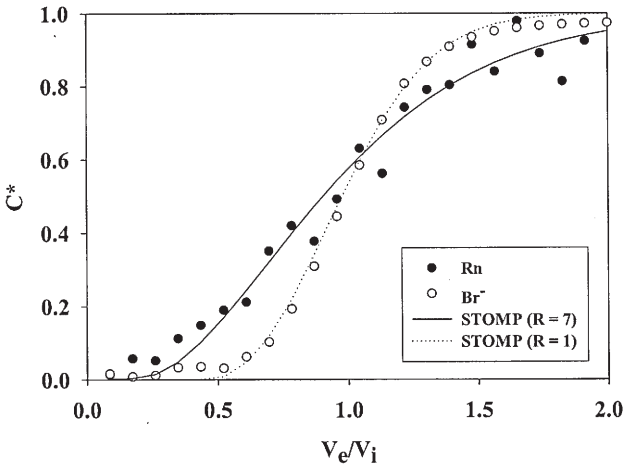

Figure 11. Pull phase breakthrough curves for a push-pull test conducted in sampling port 1 after PAM remediation. The test was conducted at a depth of 19.5 cm.

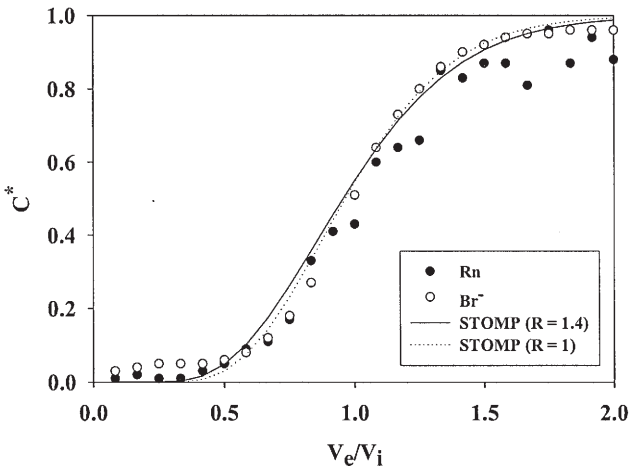

Figure 12. Pull phase breakthrough curves for a push-pull test conducted in sampling port 2 after PAM remediation. The test was conducted at a depth of 19.5 cm.

TCE partitioning, best fit R values were adjusted to account for partitioning of radon into the trapped gas using

$$R_{adj} = R_{post-TCE} - (R_{pre-TCE} - 1) \quad (9)$$

where R_{adj} is the adjusted retardation factor, $R_{post\text{-}TCE}$ is the retardation factor from a push-pull test conducted after TCE contamination, and $R_{pre\text{-}TCE}$ is the retardation factor from the push-pull test conducted prior to TCE contamination (R = 1.2, Figure 3). Adjusted retardation factors were used to calculate TCE saturations (S_n, Table 1). The best fit R = 9.4 for the push-pull test conducted after TCE contamination (Figure 4) is therefore adjusted to a value of R = 9.2. Using Equation 7, the adjusted retardation factor, and K = 50, the calculated S_n = 14.1 %. This value overestimates the volume-averaged TCE saturation of 1.2% in the sediment pack, where the TCE saturation is averaged over the ~20 cm radius of influence of this push-pull test. The reasons for this overestimation are unclear, especially in light of the subsequent static and push-pull tests that indicated that TCE sank to the bottom of the sediment pack. A heterogeneous TCE distribution with pooling toward the bottom of the sediment pack would more likely result in smaller radon retardation factors because of the reduced interfacial area between the TCE and the injection solution. This reduced interfacial area due to the geometry of the pools would limit mass transfer and could violate the assumption of equilibrium partitioning (Chrysikopoulos and Kim 2000; Willson et al. 2000). In addition, push-pull tests conducted in the fully penetrating well interrogated the entire 0 to 20 cm thickness of the PAM. Thus with a heterogeneous TCE distribution, the contribution of radon from layers of the sediment pack with either a lower TCE saturation or no TCE would serve to "dilute" the retarded radon response from layers contaminated with TCE, thus decreasing R.

Static radon samples obtained from a depth of 10 cm after TCE contamination (Figure 5) showed little change relative to pre-contamination radon concentrations (Figure 2), indicating that TCE had sunk below the 10 cm depth. The second push-pull test in the fully penetrating well (Figure 6) showed an adjusted R = 3.6, with a calculated S_n = 4.9 % (Table 1). The decrease in adjusted R values between these two push-pull tests indicates that additional TCE sank in the six months between the tests (Table 1). Although the push-pull tests may tend to overestimate S_n, the tests show that changes in retardation may indicate changes in TCE saturation distribution over time.

Results from the 15 L pull test following TCE contamination (Figures 7a and 7b) support the hypothesis that the TCE sank. The lowest radon and highest aqueous TCE concentrations were observed at a depth of 17.5 cm. The likely existence of a zone of greater S_n is shown by the decrease in radon concentrations between 3 and 5 L (Figure 7a). Assuming a cylindrical geometry, this zone is located ~11 to 14 cm from the well. Radon concentrations then increased as water from zones of lesser S_n was extracted. The decrease in radon concentrations at 7.5 cm (Figure 7a) is attributed to radon partitioning to a gas phase at the top of the sediment pack, which is consistent with a decrease in aqueous TCE concentrations at this depth. During the 15 L pull experiment it was determined that the upper 3 to 4 cm of the sediment pack was not water saturated; this was remedied by adjusting the PAM standpipe/overflow systems.

Static radon and aqueous TCE samples obtained after the 15 L pull test were obtained from a depth of 19.5 cm to account for the sinking of TCE. Radon concentrations were decreased after TCE contamination, with the greatest decreases occurring near the concentric zones of 6% and 3% TCE saturation (Figure 8a). Due to the sinking of injected TCE it is unlikely that these predicted TCE saturations were realized in the sediment pack. For example, a water sample obtained from the bottom of the sediment pack after TCE contamination contained neat TCE, supporting the hypothesis that TCE sank to the bottom of the sediment pack. The TCE injection scheme likely resulted in the highest TCE saturations in the 6% zone, with lower saturations in the 3% zone and the lowest saturations outside of the 3% zone. The highest aqueous TCE concentrations (Figure 8b) were observed in the vicinity of the lowest radon concentrations. Although aqueous TCE concentrations approaching the solubility limit were measured in these zones, calculated values of S_n (Figure 8c) were ≤ 1.4%, which were lower than expected. This is possibly due to the relationship between diffusion and the volume of water obtained from the sediment pack for each static sample (i.e., 20 mL). A radon sample obtained from directly adjacent to the TCE would have a decreased concentration (relative to the pre-TCE contamination concentration) due to partitioning of radon into TCE. However, as the sampling point moves away from the TCE, the emanation of radon from the sediment attenuates the effect of radon partitioning. A 20 mL sample interrogates a radius of ~2.3 cm, assuming a spherical shape. If TCE were not present within this sample radius, or if only a portion of the interrogated sediment was contaminated, the effect of partitioning on the observed radon concentration would be lessened. The nonlinear relationship between radon concentration and S_n (Equation 4) could also result in an underestimation of S_n. For example, a decrease in radon concentration in a sampling port from 200 to 100 pCi/L after TCE contamination would result in a calculated S_n = 2.0%. However, if the sample containing radon at 100 pCi/L contained two equal

volumes of water with 50 and 150 pCi/L, respectively, then calculating S_n individually for each of the volumes would result in calculated S_n values of 6.0 and 0.67%, with an average S_n = 3.3%. These phenomena could result in an underestimation of the TCE saturation in the sediment pack, as is evident in Figure 8c. The static method is therefore sensitive to sample size in a heterogeneous DNAPL distribution.

Figures 8a and 9a show that static radon concentrations at 19.5 cm increased in some locations after remediation, with the greatest increases occurring near the concentric zones of injected TCE. However, radon concentrations also decreased in some portions of the sediment pack. Aqueous TCE concentrations were decreased after remediation (Figure 9b), with concentrations <5 mg/L across the majority of the PAM. A comparison of calculated S_n (Figures 8c and 9c) shows a decrease after remediation in the zones of highest S_n prior to remediation. Also noted is an increase in S_n in the vicinity of x = 20 cm, y = 40 cm. The decrease in radon concentrations and resulting increased values of S_n in this vicinity could be due to the movement of TCE (during remediation). However, the presence of relatively low (<5 mg/L) concentrations of aqueous TCE in this vicinity may indicate a change in sediment pack physical properties during remediation causing localized decreases in radon concentrations. The creation of localized preferential flowpaths during remediation could increase porosity and reduce the equilibrium radon concentration (Equation 4).

A change in sediment pack physical properties is indicated by a comparison of the results from the push-pull tests conducted in the fully penetrating well before (Figures 4 and 6) and after remediation (Figure 10). The normalized bromide breakthrough curves from the post-remediation test have a greater dispersion than those from the pre-remediation tests, possibly due to the creation of preferential flowpaths resulting from the pumping of more than 1200 L of tap water and ethanol solution through the sediment pack during remediation. Preferential flowpaths and a resulting increase in porosity could decrease the travel distance of the injection solution during the push-pull test, which would result in increased dispersion in pull-phase breakthrough curves (Schroth et al. 2000). The simulation results provided poor fits to the post-remediation push-pull test normalized bromide and radon breakthrough curves, likely resulting from preferential flowpaths. However, even with the increased dispersion of the normalized bromide and radon breakthrough curves, radon retardation was not evident in this push-pull test. This supports the contention that the majority of the TCE was removed by the end of the remediation activities.

The static test results after remediation, methanol-extracted TCE concentrations <1 mg/L from core samples obtained adjacent to the fully penetrating well, and the gross mass balance on TCE provide additional evidence that the majority of the TCE was removed from the sediment pack by the end of remediation. However, two push-pull tests conducted at a depth of 19.5 cm in sampling ports 1 and 2 (Figures 11 and 12) highlight the influence of sample size and location on push-pull test results and the continued presence of TCE at the bottom of the sediment pack after remediation. These two push-pull tests had a radius of influence of ~9 cm. For sampling port 1 the adjusted R = 6.8 resulted in a calculated S_n = 10.4% (Table 1), indicating the existence of a "pocket" of higher S_n that was not detected by the push-pull test conducted in the fully penetrating well after remediation. Conversely, for sampling port 2 the adjusted R = 1.2 resulted in a calculated S_n = 0.4%, indicating that little TCE remained in the vicinity of this sampling port.

These results show that push-pull test location in a heterogeneous TCE distribution can be critical in the calculation of S_n. Moreover, a comparison of the push-pull test conducted in the fully penetrating well after remediation with the push-pull test conducted in sampling port 1 highlights the sensitivity of the method to both sample size (i.e., volume of injection solution) and test design. In this case the two tests used different volumes of injection solution (10 L vs. 1.2 L). In addition, the test in the fully penetrating well interrogated the entire thickness of the PAM, while the test in sampling port 1 was focused at the bottom of the sediment pack. The two tests, although conducted within a horizontal distance of 5 cm of each other, interrogated different volumes of the sediment pack, with the 10 L push-pull test not showing clear evidence for any remaining "pockets" of TCE. In contrast, the 1.2 L push-pull test, by nature of its location at the bottom of the sediment pack and smaller volume of injection solution, interrogated a smaller portion of the sediment pack with a greater S_n.

Conclusions

The results of the laboratory and modeling studies show that static and push-pull methods using naturally occurring radon as a partitioning tracer have the potential to characterize DNAPL saturations in the subsurface. These methods can be applied at contaminated field sites using existing monitoring wells. Radon has the potential benefit of being an in situ partitioning tracer and can be easily sampled using standard sampling techniques and liquid scintillation analysis. However, the application of these methods to characterizing field sites with heterogeneous DNAPL distributions is complicated by the methods' sensitivity to test location, sample size, and test design. The static method is influenced by spatial changes in aquifer properties and DNAPL saturations. Sample size can also critically influence results from static and push-pull tests. If DNAPL is heterogeneously distributed in the aquifer, static samples with different volumes may provide different estimates of DNAPL saturation. Similarly, a push-pull test conducted with a smaller volume of injection solution may yield a radon retardation factor different from a test conducted with a larger volume of injection solution at the same location. Test design can also influence push-pull test results through the selection of a specified thickness of an aquifer over which to conduct the test. When DNAPL is heterogeneously distributed (e.g., in a layered aquifer), push-pull tests can be performed using inflatable packers to isolate a suspected zone of DNAPL contamination. Tests conducted over the entire saturated thickness of the aquifer in the same well could yield a lesser retardation factor due to the contribution of higher radon concentrations from less contaminated portions of the aquifer. The sensitivity of the static

and push-pull methods to these factors presents challenges to the application of these methods at field sites. The static and push-pull methods have the potential to provide quantitative information on changes in DNAPL saturations as a result of remediation. However, further study of the influence of these factors on the ability of the methods to quantify DNAPL saturations is warranted.

Acknowledgments

This work was funded by the U.S. Department of Energy Environmental Management Science Program (project no. 60158). We thank Dr. Alan Fryar and two anonymous reviewers for their comments and suggestions. We also thank Mike Cantaloub, Jennifer Field, Ralph Reed, Adisorn Tovanabootr, Mark Humphrey, and Jesse Jones for assistance with laboratory and analytical activities, and Martin Schroth and Mark White for assistance with STOMP.

Editor's Note: The use of brand names in peer-reviewed papers is for identification purposes only and does not constitute endorsement by the authors, their employers, or the National Ground Water Association.

References

Adloff, J., and R. Guillaumont. 1993. *Fundamentals of Radiochemistry*. Boca Raton, Florida: CRC Press.

Annable, M.D., P.S.C. Rao, K. Hatfield, W.D. Graham, A.L. Wood, and C.G. Enfield. 1998. Partitioning tracers for measuring residual NAPL: Field-scale test results. *Journal of Environmental Engineering* 124, no. 6: 498–503.

Cable, J.E., G.C. Bugna, W.C. Burnett, and J.P. Chanton. 1996. Application of ^{222}Rn and CH_4 for assessment of groundwater discharge to the coastal ocean. *Limnology and Oceanography* 41, no. 6: 1347–1353.

Cantaloub, M. 2001. Aqueous-organic partition coefficients for radon-222 and their application to radon analysis by liquid scintillation methods. Master's thesis, Department of Civil, Construction and Environmental Engineering, Oregon State University.

Chrysikopoulos, C.V., and T. Kim. 2000. Local mass transfer correlations for nonaqueous phase liquid pool dissolution in saturated porous media. *Transport in Porous Media* 38, 167–187.

Clever, H.L. 1979. *Solubility Data Series, Volume 2*. New York: Pergamon Press.

Cohen, R.M., and J.W. Mercer. 1993. *DNAPL Site Evaluation.* Boca Raton, Florida: CRC Press.

Davis, B.M., J.D. Istok, and L. Semprini. 2002. Push-pull partitioning tracer tests using radon-222 to quantify non-aqueous phase liquid contamination. *Journal of Contaminant Hydrology* 58, 129–146.

Dwarakanath, V., N. Deeds, and G.A. Pope. 1999. Analysis of partitioning interwell tracer tests. *Environmental Science & Technology* 33, no. 21: 3829–3836.

Field, J.A., and T.E. Sawyer. 2000. High performance liquid chromatography-diode array detection of trichloroethene and aromatic and aliphatic anionic surfactants used for surfactant-enhanced aquifer remediation. *Journal of Chromatography A* 893, 253–260.

Fry, V.A., J.D. Istok, L. Semprini, K.T. O'Reilly, and T.E. Buscheck. 1995. Retardation of dissolved oxygen due to a trapped gas in porous media. *Ground Water* 33, no. 3: 391–398.

Gelhar, L.W., and M.A. Collins. 1971. General analysis of longitudinal dispersion in nonuniform flow. *Water Resources Research* 7, no. 6: 1511–1521.

Gottipati, S. 1996. Radon-222 as a tracer for performance assessment of NAPL remediation technologies in the saturated zone: An experimental investigation. Master's thesis, Department of Civil, Construction and Environmental Engineering, Oregon State University.

Hamada, T., and T. Komae. 1998. Analysis of recharge by paddy field irrigation using ^{222}Rn concentration in groundwater as an indicator. *Journal of Hydrology* 205, 92–100.

Hess, C.T., J. Michel, T.R. Horton, H.M. Prichard, and W.A. Coniglio. 1985. The occurrence of radioactivity in public water supplies in the United States. *Health Physics* 48, no. 5: 553–586.

Hopkins, O.S. 1995. Radon-222 as an indicator for nonaqueous phase liquids in the saturated zone: Developing a detection technology. Master's thesis, Department of Civil, Construction and Environmental Engineering, Oregon State University.

Humphrey, M.D. 1992. Experimental design of physical aquifer models for evaluation of groundwater remediation strategies. Master's thesis, Department of Civil, Construction and Environmental Engineering, Oregon State University.

Hunkeler, D., E. Hoehn, P. Höhener, and J. Zeyer. 1997. 222-Rn as a partitioning tracer to detect diesel fuel contamination in aquifers: Laboratory study and field observations. *Environmental Science & Technology* 31, no. 11: 3180–3187.

Istok, J.D., and M.D. Humphrey. 1995. Laboratory investigation of buoyancy-induced flow (plume sinking) during two-well tracer tests. *Ground Water* 33, no. 4: 597–604.

Jin, M., M. Delshad, V. Dwarakanath, D.C. McKinney, G.A. Pope, K. Sepehrnoori, and C.E. Tilburg. 1995. Partitioning tracer test for detection, estimation, and remediation performance assessment of subsurface nonaqueous phase liquids. *Water Resources Research* 31, no. 5: 1201–1211.

Lindsey, K.A., and G.K. Jaeger. 1993. Geologic setting of the 100-HR-3 operable unit, Hanford site, south-central Washington. WHC-SD-EN-TI-132, Rev. 0. Richland, Washington: Westinghouse Hanford Co.

Mercer, J.W., and R.M. Cohen. 1990. A review of immiscible fluids in the subsurface: Properties, models, characterization and remediation. *Journal of Contaminant Hydrology* 6, 107–163.

National Research Council. 1999. *Risk Assessment of Radon in Drinking Water*. Washington, D.C.: National Academy Press.

Nelson, N.T., and M.L. Brusseau. 1996. Field study of the partitioning tracer method for detection of dense nonaqueous phase liquid in a trichloroethene-contaminated aquifer. *Environmental Science & Technology* 30, no. 9: 2859–2863.

Nelson, N.T., M. Oostrom, T.W. Wietsma, and M.L. Brusseau. 1999. Partitioning tracer method for the in situ measurement of DNAPL saturation: Influence of heterogeneity and sampling method. *Environmental Science & Technology* 33, no. 22: 4046–4053.

Schroth, M.H., J.D. Istok, and R. Haggerty. 2000. In situ evaluation of solute retardation using single-well push-pull tests. *Advances in Water Resources* 24, 105–117.

Schwille, F. 1988. Translated by J.F. Pankow. *Dense Chlorinated Solvents in Porous and Fractured Media.* Chelsea, Michigan: Lewis Publishers.

Semprini, L., K. Broholm, and M. McDonald. 1993. Radon-222 deficit for locating and quantifying NAPL contamination in the subsurface. *EOS Transactions American Geophysical Union* 76, F276.

Semprini, L., M. Cantaloub, S. Gottipati, O. Hopkins, and J. Istok. 1998. Radon-222 as a tracer for quantifying and monitoring NAPL remediation. In *Nonaqueous-Phase Liquids,* ed. G.B. Wickramanayake and R.E. Hinchee, 137–142. Columbus, Ohio: Battelle Press.

Semprini, L., O.S. Hopkins, and B.R. Tasker. 2000. Laboratory, field and modeling studies of radon-222 as a natural tracer for monitoring NAPL contamination. *Transport in Porous Media* 38, 223–240.

Snow, D.D., and R.F. Spalding. 1997. Short-term aquifer residence times estimated from ^{222}Rn disequilibrium in artifi-

cially recharged ground water. *Journal of Environmental Radioactivity* 37, 307–325.

White, M.D., and M. Oostrom. 2000. STOMP: Subsurface Transport Over Multiple Phases, Version 2.0, User's Guide. PNNL-12034. Richland, Washington: Pacific Northwest National Laboratory.

Willson, C.S., O. Pau, J.A. Pedit, and C.T. Miller. 2000. Mass transfer rate limitation effects on partitioning tracer tests. *Journal of Contaminant Hydrology* 45, 79–97.

Wilson, R.D., and D.M. Mackay. 1995. Direct detection of residual nonaqueous phase liquid in the saturated zone using SF_6 as a partitioning tracer. *Environmental Science & Technology* 29, no. 5: 1255–1258.

Young, C.M., R.E. Jackson, M. Jin, J.T. Londergan, P.E. Mariner, G.A. Pope, F.J. Anderson, and T. Houk. 1999. Characterization of a TCE DNAPL zone in alluvium by partitioning tracers. *Ground Water Monitoring & Remediation* 19, no. 1: 84–94.